Macromolecules

Article

pubs.acs.org/Macromolecules

Enhanced Cross-Linked Density by Annealing on Fluorinated Polymers Synthesized via Initiated Chemical Vapor Deposition To Prevent Surface Reconstruction

Jose Luis Yagüe and Karen K. Gleason*

Department of Chemical Engineering, Massachusetts Institute of Technology, Cambridge, Massachusetts 02139, United States

Supporting Information

ABSTRACT: Thin films of 1*H*,1*H*,2*H*,2*H*-perfluorodecyl acrylate copolymerized with the cross-linker divinylbenzene (p(PFDA-*co*-DVB)) were synthesized via initiated chemical vapor deposition (iCVD). The vapor deposited approach is significant as the fluorinated monomer and hydrocarbon cross-linker lack a common solvent. Changes in physical and chemical properties in the copolymers before and after an annealing treatment were characterized by Fourier transform infrared spectroscopy (FTIR), atomic force microscopy (AFM), contact angle (CA) measurements with water and mineral oil, X-ray diffraction (XRD), and nanoindentation. Cross-linking results in lower CA hysteresis than measured for the iCVD p(PFDA) homopolymer. Furthermore, annealing improves the extent of reaction of the vinyl bonds on the DVB units incorporated into the film. This further enhancement in the cross-linking density is correlated with an additional reduction in the CA hysteresis observed after annealing of the p(PFDA-*co*-DVB) films. CA hysteresis values with water as low as 5° were achieved while maintaining advancing angles $\theta > 130°$. For mineral oil, CA hysteresis was found to be lower than 1° with $\theta > 85°$. The cross-linking is concluded to provide a steric barrier to the reconstruction of the surface fluorinated groups when switching between dry and wet conditions and is a primary factor in the observed reduction in CA hysteresis.

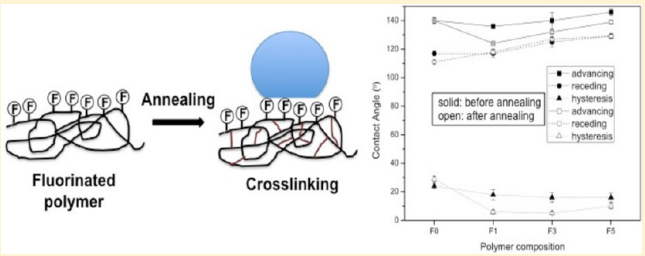

1. INTRODUCTION

Fluorinated polymers are desired for their outstanding chemical and physical properties, including a low coefficient of friction, low dielectric constant, high thermal stability, high gas permeability, and flame-retardant behavior.[1−5] Nonetheless, the primary application of fluorinated polymers derives from their hydrophobic character due to the low energy surface of the $-CF_2-$ and $-CF_3$ groups, 18 and 6 mN/m respectively.[6] The wetting properties of the fluorinated coating depend on the molecular ordering at the surface.[7,8] In the dry state, fluorine groups segregate to the surface to lower the surface energy. Angle-resolved XPS experiments have confirmed that the F/C ratio at the surface is higher than in the bulk.[9] Exposure of the surface to water is a driving force for the fluorinated groups to reorder into the bulk of the film, which reduces the hydrophobic character of the surface and thus contributes to increase the hysteresis in the contact angle (CA) behavior of water.[10] Hysteresis is the difference between the advancing and the receding CA and can be caused by surface roughness, heterogeneity of the solid surface, dissolved substances into the liquid, line tensions, and/or energy dissipation.[11] Obtaining surfaces with low CA hysteresis is desirable for many applications, including self-cleaning surfaces, ice adhesion reduction, or water condensation.[12−14] Creating chemical and physical heterogeneities are the most common approaches to modify the hysteresis. Microtextured surfaces can result in superhydrophobic surfaces. However, hysteresis depends on the wetting state of the system. Wenzel state enhances pinning of the droplet, while Cassie state reduces the CA hysteresis.[15] Additionally, crystallization can act as a barrier for surface reconstruction for fluorinated films and thus decreasing the hysteresis.[16] Enhancing the crystallinity and controlling the surface topography in fluorinated films has resulted in CA hysteresis as low as 5°.[17] Nonetheless, not all the polymers happen to crystallize, nor in all applications is crystallinity desirable. Therefore, obtaining surfaces with low CA hysteresis behavior independently of the roughness and without requiring crystallinity represents an important milestone to develop materials with improved water shedding properties.

Initiated chemical vapor deposition (iCVD) of the 1*H*,1*H*,2*H*,2*H*-perfluorodecyl acrylate (PFDA) monomer has successfully been used to develop fluorinated coatings with superhydrophobic properties.[18] iCVD is a variant of hot-wire chemical vapor deposition (HWCVD), in which an initiator decomposes at the filaments inducing a free radical polymerization, which can lead to a significant increase in the film deposition rate.[19] The iCVD method is a solvent-free technique which yields homogeneous, conformal polymer coatings with full retention of the pendant functionality of the monomeric

Received: May 22, 2013
Revised: July 18, 2013
Published: August 13, 2013

Downloaded via Chris Moua on June 22, 2020 at 14:50:57 (UTC).
See https://pubs.acs.org/sharingguidelines for options on how to legitimately share published articles.

 © 2013 American Chemical Society dx.doi.org/10.1021/ma4010633 | *Macromolecules* 2013, 46, 6548−6554

Jiangsu Favored Ex. 1026

species.[20−22] Coclite et al. demonstrated that the experimental conditions for iCVD pPFDA films can both tune the degree of crystallinity and switch the preferred orientation of the perfluorinated side chain between parallel to or perpendicular to the substrate.[23] Further studies showed that grafting PFDA polymer chains to the substrate enhances the crystallinity and alignment of the side chains perpendicular to the surface.[17] The iCVD approach enables copolymerization of two or more monomeric species. Adjusting the flow rates of monomer vapors allows for systematic control in the final composition of the copolymer.[24] While lack of a common solvent for both monomers can be a synthesis challenge for traditional polymerization, solubility characteristics are not a limited factor when the monomers are delivered through the vapor phase. Thus, iCVD can produce novel compositions. Indeed in the present work, we readily synthesize copolymers by iCVD from the fluorinated monomer PFDA with the hydrocarbon monomer divinylbenzene (DVB) (p(PFDA-*co*-DVB)) over the entire compositional range. The DVB acts as a cross-linker when both vinyl bonds are reacted. Since complete reaction of the DVB is not observed upon iCVD growth,[25] the chemical and physical properties in the current study are compared before and after annealing. We demonstrate that the DVB cross-linker and the annealing lower the CA hysteresis of the copolymers by creating a steric barrier to the surface reconstruction of the fluorinated iCVD films between their dry and wet states without inducing a crystalline state and independently of the surface roughness.

2. EXPERIMENTAL PART

2.1. Materials. *tert*-Butyl peroxide (TBPO) (98%, Aldrich), 1*H*,1*H*,2*H*,2*H*-perfluorodecyl acrylate (PFDA) (97%, Aldrich), and divinylbenzene (DVB) (80%, Aldrich) were used as received.

2.2. Experimental Setup. The polymerizations were conducted in a custom-design cylindrical reactor (diameter 24.6 cm and height 3.8 cm). On top of the reactor laid a quartz top that allowed laser interferometry (633 nm He−Ne laser, JDS Uniphase) for in-situ film thickness monitoring. Inside the reactor, 14 parallel ChromAlloy filaments (Goodfellow) were resistively heated to 230 °C, and the stage was back-cooled at a constant temperature of 30 °C by water using a recirculating chiller/heater (Neslab RTE-7). Reactor pressure was maintained at 200 mTorr using a throttle valve (MKS Instruments). The radical initiator, TBPO, and N_2 were delivered inside the reactor through mass flow controllers (MKS Instruments). The monomers PFDA and DVB were heated in a glass jar to a temperature of 80 and 60 °C, respectively, and their flows were controlled by needle valves. The flow rates of TBPO and PFDA were kept constant at 3.2 and 0.2 sccm. For the different experiments, the flow rate of DVB was varied to 0, 0.2, 0.6, and 1 sccm, and a patch flow of N_2 was introduced to keep a total flow of 5 sccm. These samples are denoted as F0, F1, F3, and F5, respectively, where integer in the label represents the ratio of DVB to PFDA in the inlet reactants (Table 1). After deposition samples were annealed at 80 °C for 30 min.

Table 1. Nomenclature and Details of the Flow Rates during the Polymerizations

	flow rate (sccm)			
sample	PFDA	DVB	TBPO	N_2
F0	0.2	0	3.2	1.6
F1	0.2	0.2	3.2	1.4
F3	0.2	0.6	3.2	1.0
F5	0.2	1.0	3.2	0.6

2.3. Characterization. Variable-angle ellipsometric spectroscopy (VASE, M-2000, J.A. Woollam) was used to measure film thicknesses. All thickness measurements were performed at a 70° incidence angle using 190 wavelengths from 315 to 718 nm. A nonlinear least-squares minimization was used to fit ellipsometric data of dry films to the Cauchy−Urbach model. The thickness was obtained upon convergence of the algorithm. The films were grown up to a thickness of 400 nm. FTIR measurements were performed on a Nicolet Nexus 870 ESP spectrometer in normal transmission mode equipped with a MCT (mercury cadmium tellurium) detector and KBr beamsplitter. Spectra were acquired over the range of 400−4000 cm^{-1} with a 4 cm^{-1} resolution for 256 scans. All spectra were baseline-corrected. CA measurements were performed using a goniometer equipped with an automated dispenser (Model 500, Rame-Hart). Advancing and receding were measured using the sessile drop method, depositing a droplet of 1 μL on the surface. The advanced CA was the largest angle obtained and the receding CA the smallest one. AFM images were acquired using a scanning probe microscope (Digital Instruments, Dimension 3100) in tapping mode using a conical gold-coated silicon tip. Crystallinity of the samples was studied by XRD. The XRD measurements were carried out on a Scintag $\theta-\theta$ diffractometer with a Cu Kα radiation (1.541 867 Å) at 40 kV and 44 mA. Data were collected in continuous mode at 3° min^{-1}, with a step size of 0.02°. The scans were taken in symmetrical reflection geometry. Mechanical properties of the film were measured by nanoindentation (Nanovea) on 1 μm thick coatings deposited on silicon substrates. The nanoindentation depth was limited to the first 10% of the overall coating thickness in order to avoid substrate effects. A Berkovich-type tip was used having a radius <10 nm. The elastic moduli were calculated from the slope of the unloading curve of the load−displacement graph, while the hardness values were calculated from the ratio of the depth at maximum load to the indent area as the tip penetrate into the coating with knowledge of the exact tip shape.

3. EXPERIMENTAL RESULTS

Figure 1 shows the FTIR spectra of the pPFDA and pDVB homopolymer and the p(PFDA-*co*-DVB) copolymer. pPFDA

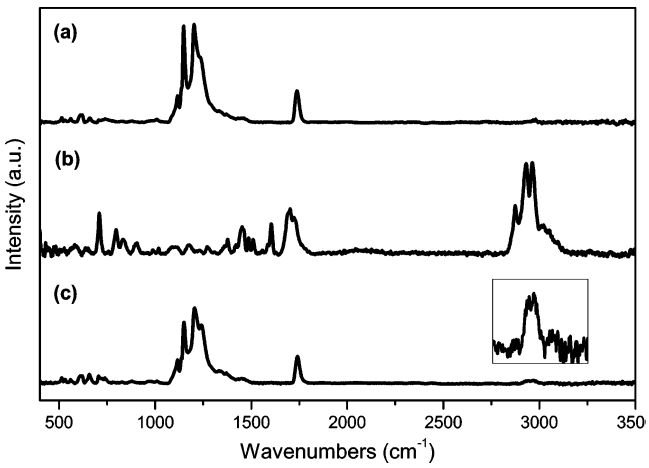

Figure 1. FTIR spectra of the pPFDA homopolymer (a), the pDVB homopolymer (b), and the p(PFDA-*co*-DVB) copolymer (c). The inset graph shows the region between 2750 and 3250 cm^{-1} of the copolymer film at expanded intensity of 220×. The bands observed resemble to the bands of the pDVB homopolymer in the same region.

homopolymer (Figure 1a) is characterized by a sharp band corresponding to the carbonyl group at 1741 cm^{-1}. In addition, the fluorinated moieties present three strong, sharp absorbance bands. The two bands at 1246 and 1207 cm^{-1} are caused by the asymmetric and symmetric stretching of the $-CF_2-$ moiety, respectively. The sharp band at 1153 cm^{-1} belongs to the

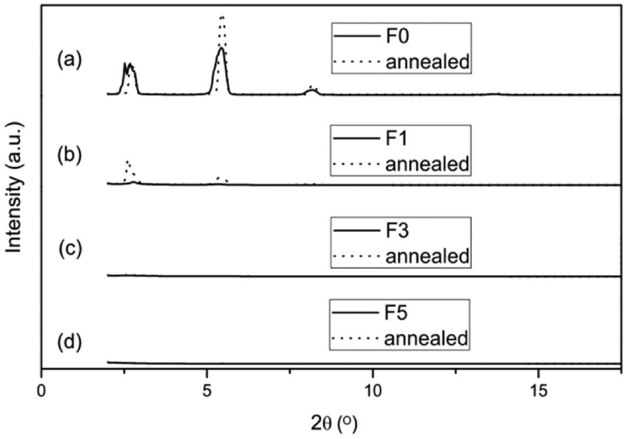

Figure 2. XRD spectra of the PFDA homopolymer, F0 (a), and the p(PFDA-*co*-DVB) copolymers F1 (b), F3 (c), and F5 (d). Solid line corresponds to the sample before annealing and dashed line after annealing. Only F0 and F1 display an increase in the crystallinity after the annealing. All the spectra were normalized to the sample thickness.

$-CF_2-CF_3$ end group.[26] Regarding the pDVB homopolymer (Figure 1b), the FTIR spectrum shows the aromatic −CH− bands between 3000 and 3100 cm^{-1}, the $-CH_2-$ stretching bands between 2810 and 2890 cm^{-1}, and some other characteristic bands related to the substituted phenyl group that appear in the range 700−1000 cm^{-1}.[27−30] The band at 710 cm^{-1} is assigned to the typical stretching vibration of the phenyl group. The bands at 795 and 838 cm^{-1} correspond to the meta- and para-disubstituted aromatic ring, respectively. The copolymer (Figure 1c) presents all the characteristic bands associated with its components. It should be noted that bands corresponding to DVB are less intense than PFDA bands but can be seen readily when the CH stretching region intensity is expanded (Figure 1 inset). Thus, the FTIR results show the incorporation of the two monomers into the copolymer film and the retention of the chemical functionality from both reactants after the polymerization.

Films with four different compositions were iCVD synthesized: F0, F1, F3, and F5. Figure 2 shows the crystallinity of the as-deposited and postannealed samples. The pPFDA homopolymer, F0 (Figure 2a), presents a characteristic lamellar structure, classified as smectic B type. This aggregation involves the arrangement of bilayers with perfluorinated side chains perpendicular to the substrate, facing each other, and forming the lamellar structure parallel to the substrate.[31] The crystalline peaks at 2.8° and 5.6° at 2θ in the X-ray diffraction (XRD) spectrum correspond to a spacing of 32.4 and 16.2 Å, respectively. These distances match with the length of a double layer and a single layer of the perfluorinated side chain, respectively, corroborating the smectic B aggregation.[17] Annealing increases the intensity of peaks observed in the XRD data for F0. The observed increase can be attributed to reorganization of the polymer chain due to the thermal process,

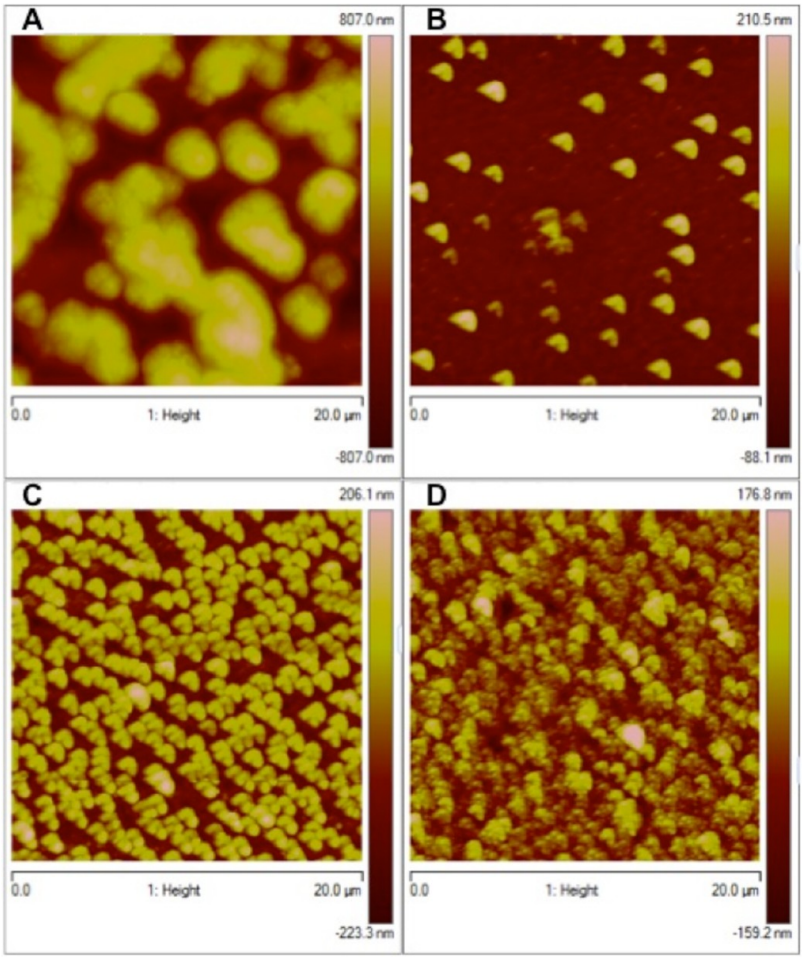

Figure 3. AFM images of the PFDA homopolymer, F0 (A), and the p(PFDA-*co*-DVB) copolymers F1 (B), F3 (C), and F5 (D) as-deposited.

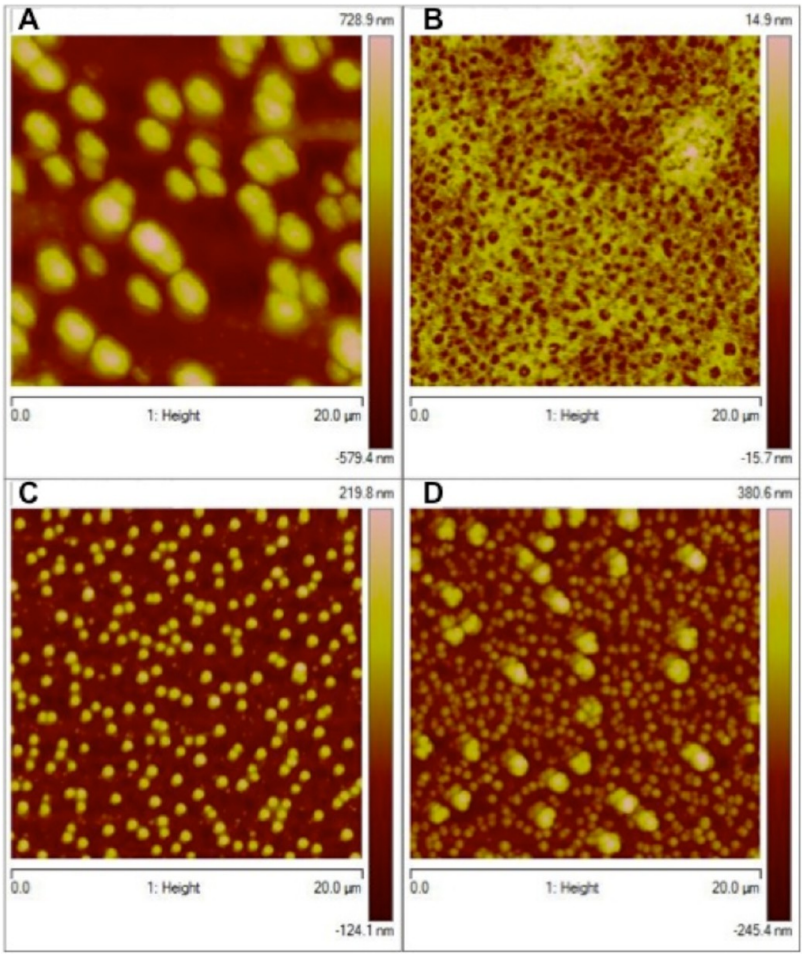

Figure 4. AFM images of the PFDA homopolymer, F0 (A), and the p(PFDA-*co*-DVB) copolymers F1 (B), F3 (C), and F5 (D) after annealing.

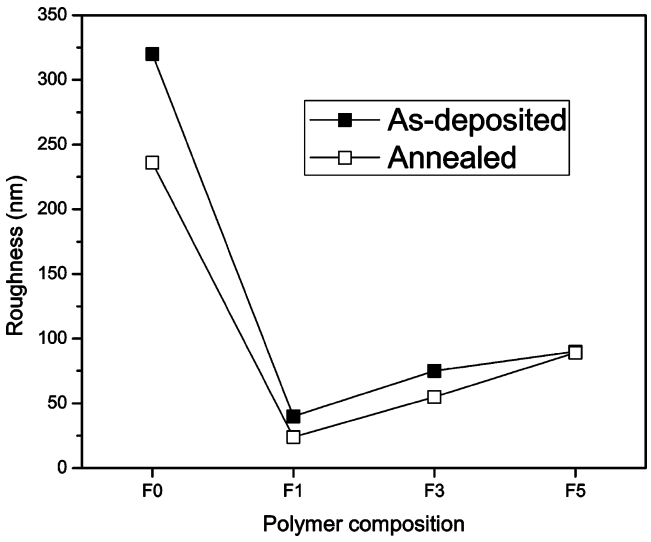

Figure 5. Roughness evolution (nm) of the polymer films as-deposited (solid symbols) and after the annealing treatment (open symbols).

which improves the crystalline structure.[32] In all as-deposited copolymer films, F1, F3, and F3, no XRD peaks are observed (Figures 2b, 2c, and 2d, respectively), indicating that these films are amorphous. Thus, the addition of the DVB cross-linker to pPFDA eliminates crystallinity in the as-deposited films. After annealing, only the copolymer with the lowest DVB content, F1, displays any crystallinity (Figure 2b). The degree of crystallinity of the annealed F1 sample is lower than that of the F0 homopolymer. Thus, incorporation of the DVB hinders the arrangement of the perfluorinated side chains into the Smetic B aggregation, leading to a loss of crystallinity.

Surface morphologies of the as-deposited films were studied by atomic force microscopy (AFM) (Figure 3). The F0 homopolymer (Figure 3a) presents large islands, characteristic of previously reported pPFDA films with crystallinity achieved at high initiator/monomer (I/M) ratio.[23] Conversely, the morphology of the copolymer samples is rather different (Figures 3b−d). The polymer aggregations found on the surface are smaller and their density increases with increasing DVB flow rate. This could be due to the formation of a higher number of nucleation sites. Nucleation is intimately related to the monomers adsorption on the surface, which in turn, depends on the P_M/P_{sat} parameter, the ratio of the vapor pressure of the monomer to the saturation vapor pressure of the monomer, equivalently to the monomer surface concentration.[33] Thus, working at the same total gas pressures, raising the flow rate of DVB increases its P_M/P_{sat} which is observed to correlate with the formation of more nucleation sites during the polymerization process. Furthermore, annealing of the films results in a decrease of the grain size depending on the DVB incorporated in the polymer chain, as observed in Figure 4. The more cross-linked are the films, the less variation in the grain size. It could be hypothesized that the DVB cross-linker density hinders the reorganization of the polymer chains and therefore

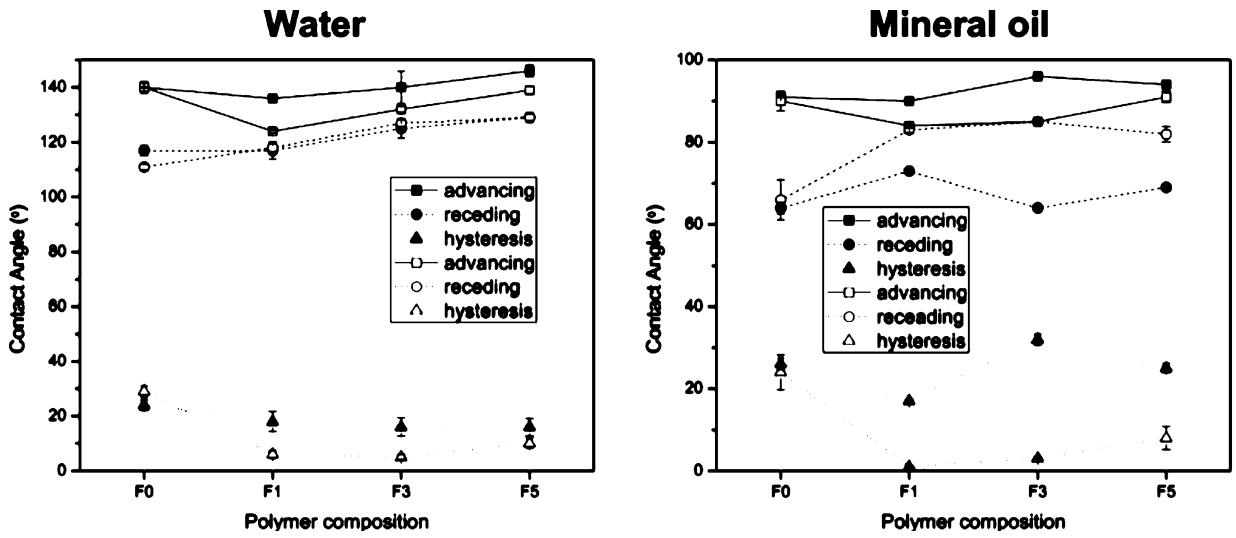

Figure 6. Advancing, receding and hysteresis of water (left) and mineral oil (right) CA of the PFDA homopolymer, F0, and the p(PFDA-*co*-DVB) copolymers corresponding to F1, F3, and F5. Solid symbols correspond to the sample before annealing and open symbols after annealing.

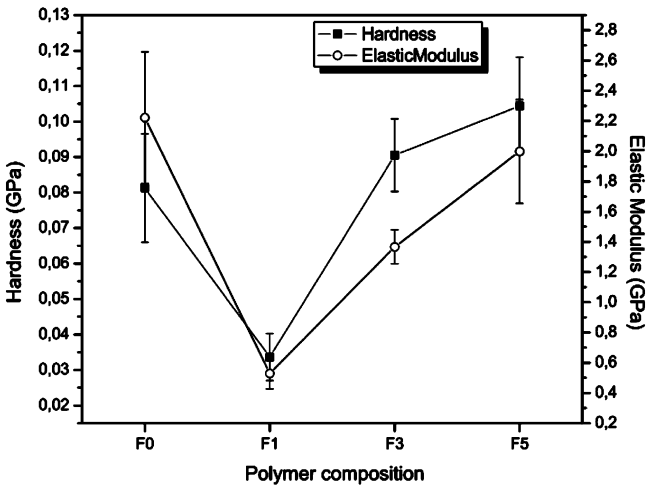

Figure 7. Hardness and elastic modulus as a function of the DVB cross-linker.

the decrease of the grain size. The change in the surface topography was also studied following the roughness variation for the different samples (Figure 5). The main difference is observed between the homo- and the copolymer samples, where the roughness decreases abruptly. The transition from the crystalline to the amorphous state entails the loss of the crystalline domains, which are characterized by large island-shape aggregations. However, as seen in the AFM images, the copolymer films show smaller and more numerous aggregations, which confers a lower roughness to the film. These results are in agreement with the change in crystallinity observed in the XRD experiments.

The cross-linking and the annealing effects on the surface wettability were evaluated by CA measurements using water and mineral oil (Figure 6). Homo- and copolymer samples present a similar hydrophobic behavior, with an advancing CA > 130°, before and after annealing. This finding suggests that both materials have a comblike structure leading to CF3 enrichment on the surface when in contact with air. The hydrocarbon nature of the cross-linker, which would increase the surface energy,[34] is not detected at the surface layer leading to similar advancing CA measurements. It should be noted, however, the decrease on the CA hysteresis due to the annealing process in the copolymerized samples. Whereas annealed copolymerized films show a CA hysteresis lower than 10°, the rest of samples present a hysteresis higher than 20°. Low CA hysteresis on fluorinated surfaces is related to the fluorine concentration on the surface. It is known that the pendant fluorinated groups of polymer chains segregate of the surface under dry conditions and reorient into the bulk when the surface is exposed to water. The reduction in the surface fluorine concentration in the wet state decreases the value of the receding CA.[35] The cross-linking of the DVB units, which is enhanced upon annealing, fixes the fluorine concentration on top of the surface. Additionally, only in the homopolymer film, F0, and in the copolymer polymer film with the lowest degree of DVB incorporation, F1, does the degree of crystallinity increases with annealing. This crystallinity represents an additional steric barrier to the reorientation of the perfluorinated functional groups.[23] Note that for copolymer sample F1 crystallinity is observable only after annealing, as no diffraction peaks are seen in the as-deposited film. Thus, the annealed sample F1 is unique in having both cross-linking and crystallinity. This annealed sample also provides the lowest CA hysteresis values for both water and mineral oil.

The degree of cross-linking in pDVB can be quantified by determining the area in the FTIR spectrum of two characteristic bands: one band at 903 cm^{-1} corresponding to the vinyl bound and the other one at 710 cm^{-1} belonging to the meta-substituted DVB ring.[25] Since these bands are not intense enough in the copolymer spectrum, the cross-linking measurement was performed over a pDVB homopolymer film (see spectra in Supporting Information, Figure S1). Cross-linking before annealing was 55% and after 68%, which corroborates the increase of cross-linking density due to the thermal treatment. Similar behavior can be observed for the mineral oil CA measurements. All samples show an advancing CA with mineral oil of around 90°. Copolymerized annealed samples present a decrease of 20° in the hysteresis obtaining values lower than 1°. Moreover, as observed in Figure 5, the roughness before and after the annealing can be considered to be within the same order for the copolymers, which means

that the decrease of the CA hysteresis is independent of the surface morphology. Thus, the driving force to obtain this low hysteresis is based primarily on the improvement of the reduction in the surface reconstruction of the fluorine groups, which is due to the formation of a steric barrier against molecular reorientation produced by the incorporation of cross-linkable groups.

Mechanical properties of the thin films were studied using nanoindentation (Figure 7). Contrary to expectations, the pPFDA homopolymer shows high values for the Young's modulus (Y) and hardness (H) in comparison to p(PFDA-*co*-DVB) copolymers. This result may be explained by the fact that the homopolymer presents a highly crystalline structure.[36,37] The secondary bonds formed due to the orientation of the polymer chains create a cross-linked effect increasing the stiffness and strength of the polymer. The introduction of DVB leads to a loss of crystallinity and, thus, a decrease in the Y and H values for the F1 sample. Nonetheless, increasing the amount of DVB cross-linker in the polymer background causes the boost of the mechanical properties of the thin films because of the bonds formed among chains.

4. CONCLUSIONS

In this work, we have demonstrated the synthesis of p(PFDA-*co*-DVB) copolymer thin films via iCVD showing hydrophobic and oleophobic properties. In the as-deposited films, the introduction of the DVB cross-linker entails a loss of crystallinity in comparison with the pPFDA homopolymer as well as a reduction in the grain size of the particles aggregated on the surface, resulting in films with lower roughness. The mechanical properties of the films increase with the amount of cross-linker incorporated in the copolymer; however, the homopolymer shows comparable values due to its crystallinity state. Furthermore, an annealing treatment has been performed to the films. The annealing produced crystallinity in only one of the copolymer samples, F1, which possesses the lowest amount of DVB cross-linker. The CA hysteresis after the annealing process for the copolymer films has decreased significantly, obtaining values as low as 5° for water and lower than 1° for mineral oil droplets. The annealing leads to a higher cross-linking density through reaction of the pendant vinyl bonds of pDVB. Cross-linking acts as a steric barrier for the reorganization of the fluorinated groups on the surface. The introduction of the cross-linker and the annealing in the polymerization process of fluorocompounds result in low-energy surfaces showing no or little segregation without the need of inducing crystallinity. These smooth, chemically stable, and low-hysteresis thin films are excellent candidates for applications demanding low CA hysteresis with fluids having surface energies between those for water and those for mineral oil.

■ ASSOCIATED CONTENT

Ⓢ Supporting Information

FT-IR spectra. This material is available free of charge via the Internet at http://pubs.acs.org.

■ AUTHOR INFORMATION

Corresponding Author

*E-mail: kkg@mit.edu (K.K.G.).

Notes

The authors declare no competing financial interest.

■ ACKNOWLEDGMENTS

The authors gratefully acknowledge the support of the Masdar Institute for funding this research.

■ REFERENCES

(1) Suzuki, M.; Saotome, Y.; Yanagisawa, M. *Thin Solid Films* **1988**, *160*, 453−462.
(2) Maier, G. *Prog. Polym. Sci.* **2001**, *26*, 3−65.
(3) Kang, J. W.; Kim, J. P.; Lee, W. Y.; Kim, J. S.; Lee, J. S.; Kim, J. J. *J. Lightwave Technol.* **2001**, *19*, 872−875.
(4) Tanaka, K.; Kita, H.; Okano, M.; Okamoto, K. *Polymer* **1992**, *33*, 585−592.
(5) Errifai, I.; Jama, C.; Le Bras, M.; Delobel, R.; Gengembre, L.; Mazzah, A.; De Jaeger, R. *Surf. Coat. Technol.* **2004**, *180*, 297−301.
(6) Zisman, W. A. In *Relation of the Equilibrium Contact Angle to Liquid and Solid Constitution*; American Chemical Society: Washington, DC, 1964; Vol. *43*, pp 1−51.
(7) Genzer, J.; Sivaniah, E.; Kramer, E. J.; Wang, J. G.; Korner, H.; Xiang, M. L.; Char, K.; Ober, C. K.; DeKoven, B. M.; Bubeck, R. A.; Chaudhury, M. K.; Sambasivan, S.; Fischer, D. A. *Macromolecules* **2000**, *33*, 1882−1887.
(8) Corpart, J. M.; Girault, S.; Juhue, D. *Langmuir* **2001**, *17*, 7237−7244.
(9) Mao, Y.; Gleason, K. K. *Macromolecules* **2006**, *39*, 3895−3900.
(10) Synytska, A.; Appelhans, D.; Wang, Z. G.; Simon, F.; Lehmann, F.; Stamm, M.; Grundke, K. *Macromolecules* **2007**, *40*, 297−305.
(11) Butt, H.-J.; Graf, K.; Kappl, M. In *Contact Angle Phenomena and Wetting*; Wiley-VCH Verlag GmbH & Co. KGaA: Weinheim, 2004; pp 118−144.
(12) Bhushan, B.; Jung, Y. C.; Koch, K. *Philos. Trans. R. Soc., A* **2009**, *367*, 1631−1672.
(13) Kulinich, S. A.; Farzaneh, M. *Appl. Surf. Sci.* **2009**, *255*, 8153−8157.
(14) Wier, K. A.; McCarthy, T. J. *Langmuir* **2006**, *22*, 2433−2436.
(15) Lafuma, A.; Quere, D. *Nat. Mater.* **2003**, *2*, 457−460.
(16) Wang, J. G.; Mao, G. P.; Ober, C. K.; Kramer, E. J. *Macromolecules* **1997**, *30*, 1906−1914.
(17) Coclite, A. M.; Shi, Y. J.; Gleason, K. K. *Adv. Mater.* **2012**, *24*, 4534−4539.
(18) Ma, M. L.; Gupta, M.; Li, Z.; Zhai, L.; Gleason, K. K.; Cohen, R. E.; Rubner, M. F.; Rutledge, G. C. *Adv. Mater.* **2007**, *19*, 255−259.
(19) Martin, T. P.; Lau, K. K. S.; Chan, K.; Mao, Y.; Gupta, M.; O'Shaughnessy, A. S.; Gleason, K. K. *Surf. Coat. Technol.* **2007**, *201*, 9400−9405.
(20) Tenhaeff, W. E.; Gleason, K. K. *Adv. Funct. Mater.* **2008**, *18*, 979−992.
(21) Ozaydin-Ince, G.; Coclite, A. M.; Gleason, K. K. *Rep. Prog. Phys.* **2012**, *75*, 016501.
(22) Yagüe, J. L.; Coclite, A. M.; Petruczok, C.; Gleason, K. K. *Macromol. Chem. Phys.* **2013**, *214*, 302−312.
(23) Coclite, A. M.; Shi, Y. J.; Gleason, K. K. *Adv. Funct. Mater.* **2012**, *22*, 2167−2176.
(24) Yagüe, J. L.; Gleason, K. K. *Soft Matter* **2012**, *8*, 2890−2894.
(25) Petruczok, C. D.; Yang, R.; Gleason, K. K. *Macromolecules* **2013**, *46*, 1832−1840.
(26) Gupta, M.; Gleason, K. K. *Langmuir* **2006**, *22*, 10047−10052.
(27) Bartholin, M.; Boissier, G.; Dubois, J. *Makromol. Chem.* **1981**, *182*, 2075−2085.
(28) Boguslavsky, Y.; Margel, S. *J. Colloid Interface Sci.* **2008**, *317*, 101−114.
(29) Ji, H. F.; Wang, S. P.; Yang, X. L. *Polymer* **2009**, *50*, 133−140.
(30) Hasegawa, J.; Kanamori, K.; Nakanishi, K.; Hanada, T. *C. R. Chim.* **2010**, *13*, 207−211.
(31) Honda, K.; Morita, M.; Otsuka, H.; Takahara, A. *Macromolecules* **2005**, *38*, 5699−5705.
(32) Rottele, A.; Thurn-Albrecht, T.; Sommer, J. U.; Reiter, G. *Macromolecules* **2003**, *36*, 1257−1260.

(33) Lau, K. K. S.; Gleason, K. K. *Macromolecules* **2006**, *39*, 3688−3694.
(34) Kim, B. G.; Sohn, E. H.; Lee, J. C. *Macromol. Chem. Phys.* **2007**, *208*, 1011−1019.
(35) Synytska, A.; Appelhans, D.; Wang, Z. G.; Simon, F.; Lehmann, F.; Stamm, M.; Grundke, K. *Macromolecules* **2007**, *40*, 1774−1774.
(36) Cadek, M.; Coleman, J. N.; Barron, V.; Hedicke, K.; Blau, W. J. *Appl. Phys. Lett.* **2002**, *81*, 5123−5125.
(37) Starkweather, H. W.; Moore, G. E.; Hansen, J. E.; Roder, T. M.; Brooks, R. E. *J. Polym. Sci.* **1956**, *21*, 189−204.